arXiv:astro-ph/9706275v1 27 Jun 1997

Vertical equilibrium of molecular gas in galaxies

F. Combes and J-F. Becquaert

Observatoire de Paris, DEMIRM, 61 av. de l'Observatoire, F-75014 Paris

Abstract. We present CO(1-0) and CO(2-1) observations of the two nearly face-on galaxies NGC 628 and NGC 3938, in particular cuts along the major and minor axis. The contribution of the beam-smeared in-plane velocity gradients to the observed velocity width is quite small in the outer parts of the galaxies. This allows us to derive the velocity dispersion of the molecular gas perpendicular to the plane. We find that this dispersion is remarkably constant with radius, $6 \, \mathrm{km \, s^{-1}}$ for NGC 628 and $8.5 \, \mathrm{km \, s^{-1}}$ for NGC 3938, and of the same order as the H I dispersion. The constancy of the value is interpreted in terms of a feedback mechanism involving gravitational instabilities and gas dissipation. The similarity of the CO and H I dispersions suggests that the two components are well mixed, and are only two different phases of the same kinematical gas component. The gas can be transformed from the atomic phase to the molecular phase and vice-versa several times during a z-oscillation.

Key words: Interstellar medium: kinematics and dynamics – Galaxies: individual: NGC 628 – Galaxies: individual: NGC 3938 – Galaxies: ISM – Galaxies: kinematics and dynamics – Galaxies: spiral

1. Introduction

An important diagnostic of the physical state of the interstellar medium is its large-scale velocity dispersion. This parameter is however very difficult to derive, since it is in general dominated by the contribution of the systematic velocity gradients in the beam, which are not well-known. Exactly face-on galaxies are ideal objects for this study, since the line-width can be attributed almost entirely to the z-velocity dispersion σ_v. Indeed, the systematic gradients perpendicular to the plane are expected negligible; for instance no systematic pattern associated to spiral arms have been observed in face-on galaxies (e.g. Shostak & van der Kruit 1984, Dickey et al 1990), implying that the

z-streaming motions at the arm crossing are not predominant. In an inclined galaxy on the contrary, it is very difficult to obtain the true velocity dispersion, since the systematic motions in the plane $z = 0$ (rotation, arm streaming motions) widen the spectra due to the finite spatial resolution of the observations (e.g. Garcia-Burillo et al 1993, Vogel et al 1994).

Nearly face-on galaxies have already been extensively studied in the atomic gas component, in order to derive the true H I velocity dispersion (van der Kruit & Shostak 1982, 1984, Shostak & van der Kruit 1984, Dickey et al 1990). The evolution of σ_v as a function of radius was derived: the velocity dispersion is remarkably constant all over the galaxy $\sigma_v = 6 \, \mathrm{km \, s^{-1}} = \Delta V_{FWHM}/2.35$, and only in the inner parts it increases up to $12 \, \mathrm{km \, s^{-1}}$.

The constancy of σ_v in the plane, and in particular in the outer parts of the galaxy disk, is not yet well understood; it might be related to the large-scale gas stability and to the linear flaring of the plane, as is observed in the Milky-Way (Merrifield 1992) and M31 (Brinks & Burton 1984). In the isothermal sheet model of a thin plane, where the z-velocity dispersion σ is independent of z, the height $h_g(\mathrm{r})$ of the gaseous plane, if assumed self-gravitating, is

$$h_g(r) = \frac{\sigma_g^2(r)}{2\pi G \mu_g(r)}$$

where σ_g is the gas velocity dispersion, and $\mu_g(r)$ the gas surface density. The density profile is then a sech^2 law. But to have the gas self-gravitating, we have to assume that either there is no dark matter component, or the gas is the dark matter itself (e.g. Pfenniger et al 1994). Since in general the H I surface density decreases as $1/\mathrm{r}$ in the outer parts of galaxies (e.g. Bosma 1981), a linear flaring ($h_g \propto r$) corresponds to a constant velocity dispersion with radius.

On the contrary hypothesis of the gas plane embedded in an external potential of larger scale height, where the gravitational acceleration close to the plane can be approximated by $K_z z$, the z-density profile is then a Gaussian:

$$\rho_g = \rho_{0g} e^{-\frac{1}{2}\frac{K_z z^2}{\sigma_g^2}}$$

and the characteristic height, or gaussian scale height of the gas is:

$$h_g = \frac{\sigma_g}{\sqrt{K_z}}$$

and K_z is $4\pi G\rho_0$, where $\rho_0(r)$ is the density in the plane of the total matter, stellar component plus dark matter component, in which the gas is embedded. If the dark component is assumed spherical, the density in the plane is dominated by the stellar component, which is distributed in an exponential disk. This hypothesis would predict an exponential flare in the gas, while the gas flares appear more linear than exponential (e.g. Merrifield 1992, Brinks & Burton 1983). The knowledge of their true shape is however hampered by the presence of warps. Also, the flattening of the dark matter component, and its participation to the density ρ_0 in the plane, is unknown.

As for the stability arguments, let us assume here the z-velocity dispersion comparable to the radial velocity dispersion, or at least their ratio constant with radius. The velocity dispersion of the gas component is self-regulated by dynamical instabilities. If the Toomre Q parameter for the gas

$$Q_g = \sigma_g(r)\kappa(r)/3.36G\mu_g(r) = \sigma_g(r)/\sigma_{cg}(r)$$

is lower than 1, instabilities set in, heat the medium and increase $\sigma_g(r)$ until Q_g is 1. The critical velocity dispersion σ_{cg} depends on the epicyclic frequency $\kappa(r)$ and on the gas surface density $\mu_g(r)$; assuming again an H I surface density decreasing as $1/r$ in the outer parts and a flat rotation curve, where $\kappa(r)$ also varies as $1/r$, then σ_{cg} is constant. To maintain $Q_g = 1$ all over the outer parts, σ_g should also remain constant.

However, the gas density gradient appears often steeper than $1/r$ and the Q_g parameter is increasing towards the outer parts. This has been noticed by Kennicutt (1989), who concluded that there exists some radius in every galaxy where the gas density reaches the threshold of global instability ($Q_g \approx 1$); he identifies this radius to the onset of star formation in the disk. In fact, this threshold does not occur exactly at $Q_g = 1$, but at a slightly higher value, around 1.4, which could be due to the fact that the Q criterion is a single-fluid one, which does not take into account the coupling between gas and stars.

The determination of the z-velocity dispersion in the molecular component has not yet been done. It could bring complementary insight to the H I results, since in general the center of galaxies is much better sampled through CO emission (a central H I depletion is frequent), and also the thickness of the H_2 plane can be lower by a factor 3 or 4 than the H I layer (case of MW, M31, Boulanger et al 1981). In the case of M51, an almost face-on galaxy (i=20°), the estimated σ_v determined from the CO lines is surprisingly large (up to $\sigma_v = 25$ km s^{-1}in the southern arm) once the rotation field, and even streaming-motions

are taken into account, at the beam scale. An interpretation could be that the CO lines are broadened by macroscopic opacity, i.e. cloud overlapping (Garcia-Burillo et al 1993), since such large line-widths are not observed in galaxies with less CO emission. However, one could also suspect turbulent motions, generated at large-scale by gravitational instabilities or viscous shear. The level of star formation could be another factor: as for turbulence, it generally affects the molecular component more than the HI, except for very violent events like SNe. But the finite inclination (20°) of M51 makes the discrimination between in-plane and z-dispersion very delicate. It is therefore necessary to investigate in more details this problem in exactly face-on galaxies, and determine whether there exist spatial variations of σ_v over the galaxy plane.
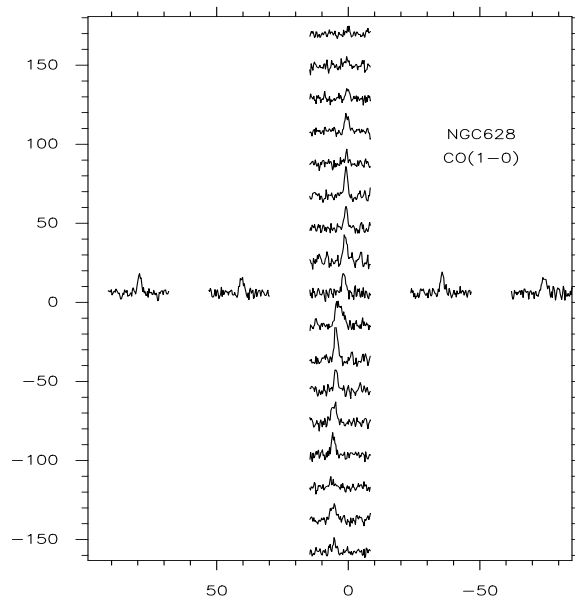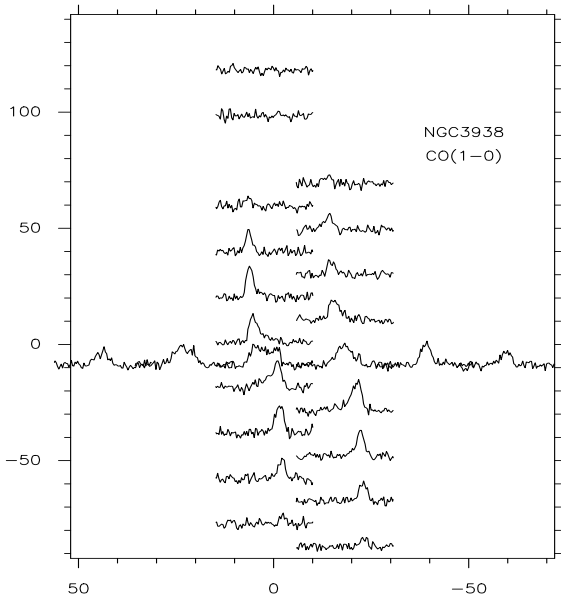

Fig. 1. Map of CO(1-0) spectra towards NGC 628. The scale in velocity is from 556 to 756 km s^{-1}, and in T$_A^*$ from -0.05 to 0.18K. The major axis has been rotated by 25° to be vertical. The offsets marked on the box are in arcsec.

In this paper we report molecular gas observations of two face-on galaxies NGC 628 (M74) and NGC 3938, in the CO(1-0), CO(2-1) and ^{13}CO lines, using the IRAM 30–m telescope. After a brief description of the galaxy parameters in section 2, and the observational parameters in section 3, we derive the amplitude and the spatial variations of σ_v perpendicular to the plane in NGC 628 and NGC 3938. Section 5 summarises and discusses the physical interpretations.

Table 1. Galaxy properties

Name	Type	Coordinates		$V_\odot$	Dist	L_B	f_{60}	f_{100}	D_{25}	PA	i	Environment
		α(1950)	δ(1950)	$km\,s^{-1}$	Mpc	$10^9\,L_\odot$	Jy		$'$	$\circ$	$\circ$	
NGC 628	Sc(s)I	01 34 0.7	15 31 55	656	10	25	20	65	10.7	25	6.5	loose group, comp. at 140 kpc
NGC 3938	Sc(s)I	11 50 13.6	44 24 07	808	10	11	4.9	22	5.4	20	11.5	Ursa Mayor Cl., no comp.< 100kpc

Fig. 2. Map of CO(1-0) spectra towards NGC 3938. The scale in velocity is from 608 to 908 $km\,s^{-1}$, and in T^*_A from -0.05 to 0.18K. The major axis has been rotated by 20° to be vertical. The offsets marked on the box are in arcsec.

2. Relevant galaxy properties

2.1. NGC 628

NGC 628 (M74) is a large (Holmberg radius $R_{Ho} = 6'$) bright face-on galaxy, with a remarkable H I extension, as large as 3.3 R_{Ho} (Briggs et al 1980). Sandage & Tamman (1975) propose a distance of 19.6 Mpc from the size of its H II regions, but most authors adopt a distance of 10 Mpc, based on a Hubble constant of 75 $km\,s^{-1}Mpc^{-1}$. At this distance, $1'$ is about 3 kpc, and our beams are 1.1 kpc and 580 pc in CO(1-0) and CO(2-1) lines respectively.

Disk morphology and star formation activity were derived by Natali et al (1992): they fit the I-band light distribution by an exponential disk of scale length 4 kpc, and a bulge of 1.5 kpc extent, which we will use below to interprete the rotation curve. NGC 628 has a very modest star

formation rate of 0.75 star/yr, which is fortunate, since violent stellar activity agitates the interstellar medium, through the formation of bubbles, jets, stellar winds, and the intrinsic or un-perturbed z-velocity dispersion could not be naturally measured.

The stellar velocity dispersion has been derived by van der Kruit & Freeman (1984): it is 60±20 $km\,s^{-1}$ at about one luminosity scale-length, and its evolution with radius is compatible with an exponential decrease, with a radial scalelength twice that of the density distribution, as expected if the stellar disk has a constant scale-height with radius. This result has been derived for several galaxies by Bottema (1993). The H I distribution has been observed at Westerbork with 14″x 48″ beam by Shostak & van der Kruit (1984) who derived an almost constant z-velocity dispersion (9-10 $km\,s^{-1}$ in the center, to 7-8 $km\,s^{-1}$ in the outer parts). Kamphuis & Briggs (1992) investigate in more details the H I outer disk with the VLA (beam 53″x 43″). They found that the inner disk of NGC 628 is relatively unperturbed, with an inclination of 6.5° and a PA of 25°, while at a radius of about 6′ (18 kpc), the plane begins to be tilted, warped and perturbed by high velocity H I clouds . These clouds could be accreting onto the outer parts, and fueling the warp.

As for the molecular component, a cross has been observed in NGC 628 by Adler & Liszt (1989) with the Kitt Peak 12m telescope (beam 1′=3 kpc), and Wakker & Adler (1995) presented BIMA interferometric observations, with a resolution of 7.1″x 11.6″ (340 x 560 pc). They showed that there might be a CO emission hole in the center, of size $\approx$ 10″, but this could be only a relative deficiency, since only 45% of the single-dish flux is recovered in the interferometric observations. The total masses derived are M(H$_2$)=2 10^9 M$_\odot$, M(HI)= 1.2 10^{10} M$_\odot$, and from the flat rotation curve V$_{rot}$=200 $km\,s^{-1}$ an indicative total mass inside two Holmberg radii (12′= 36 kpc) M$_{tot} = 3.3\ 10^{11}$ M$_\odot$, assuming a spherical mass distribution.

2.2. NGC 3938

NGC 3938 is also a nearly face-on galaxy, at about the same distance as NGC 628. Its distance derived from its corrected radial velocity (850 $km\,s^{-1}$) and a Hubble constant of 75 $km\,s^{-1}Mpc^{-1}$ is 11.3 Mpc, but Sandage & Tamman (1974) derive a distance of 19.5 Mpc from the H II
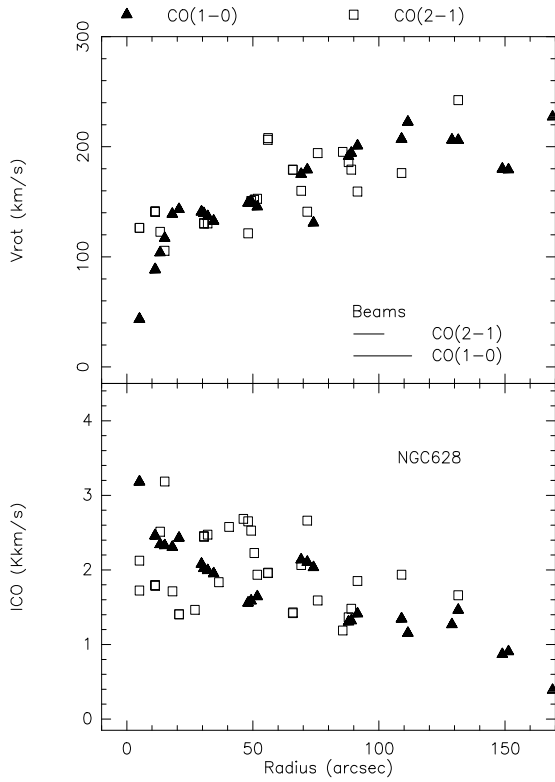
Fig. 3. top Rotation curve derived from the CO(1-0) (filled triangles) and CO(2-1) (open squares) observed points in NGC 628. The adopted inclination is 6.5°. **bottom** Radial distribution of integrated CO emission in NGC 628.
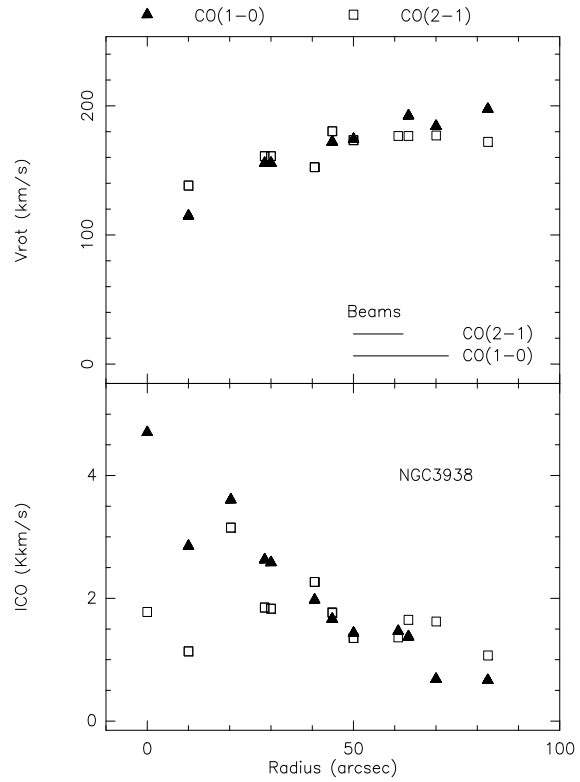
Fig. 4. top Rotation curve derived from the CO(1-0) (filled triangles) and CO(2-1) (open squares) observed points in NGC 3938. The adopted inclination is 11.5°. **bottom** Radial distribution of integrated CO emission in NGC 3938.

regions. We will adopt here a distance of 10 Mpc, to better compare with the literature, where this value is more frequently used.

Its global star formation rate is comparable to that of NGC 628, its ratio between far-infrared and blue luminosity is L_{FIR}/L_B=0.15 (while L_{FIR}/L_B=0.19 for NGC 628). The stellar velocity dispersion was measured by Bottema (1988, 1993) to be about 20 $km\,s^{-1}$ at one scale-length: its radial variation is also exponential, compatible with a constant stellar scale height.

An H I map was obtained at Westerbork with 24″x 36″ beam (1.1 x 1.7 kpc) by van der Kruit & Shostak (1982), and the z-velocity dispersion was also found almost constant with radius at a value of 10 $km\,s^{-1}$. They found no evidence of a systematic pattern of z-motions in the H I layer, in excess of 5 $km\,s^{-1}$. CO emission has been reported by Young et al (1995) towards 4 points, with a beam of 45″ (2.1 kpc), and the central line-width was 70 $km\,s^{-1}$. The total masses derived are M(H$_2$)=1.6 10^9 M$_\odot$, M(HI)= 1.6 10^9 M$_\odot$, and from the flat rotation curve V$_{rot}$=180 $km\,s^{-1}$ an indicative total mass inside two Holmberg radii

(7′= 21 kpc) M$_{tot}$ = 1.5 10^{11} M$_\odot$, assuming a spherical mass distribution.

There are some uncertainties about the inclination, as it is usual for nearly face-on galaxies. Danver (1942) adopted an inclination of i=9.5°, and van der Kruit & Shostak (1982) after fitting the H I velocity field and from the galaxy type deduce i=8°-11°. This corresponds to a maximum velocity of 200-250$km\,s^{-1}$. Bottema (1993) uses the Tully-Fisher relation established by Rubin et al (1985) to deduce a maximum rotational velocity of 150$km\,s^{-1}$, corresponding to an inclination of 15°. However, the Tully-Fisher relation has an intrinsic scatter. If we compare with NGC 628, NGC 3938 has about half the luminosity, and half the radial scale-length (the exponential scales of the disk are h$_d$=4 and 1.75kpc, and D$_{25}$ see Table 1). If we choose comparable M/L ratios, given they have the same type, and about the same star formation rate, we expect comparable maximum rotational velocities. We then adopt a compromise of V$_{max}$ ≈ 180$km\,s^{-1}$, and an inclination of i=11.5°. We note that this will not change our

conclusions about the vertical dispersions, except that the critical dispersions for stability σ_c scale as V_{max}^{-1}.

3. Observations

Most of the observations were made in August 1994 with the IRAM 30–m telescope, equipped with single side–band tuned SIS receivers for both the CO(1-0) and the CO(2-1) lines. The observations were done in good weather conditions, but the relative humidity was typical of summer time, which affected essentially the high frequency observations (the CO(2-1) line). The typical system temperatures, measured in the Rayleigh–Jeans main beam brigthness temperature (T_A^*) scale, of $350\,K$ and $1000\,K$ for the 115 and 230 GHz lines, respectively.

We used two 512 channel filterbanks, with a channel separation of $2.6\,km\,s^{-1}$ and $1.3\,km\,s^{-1}$ for the CO(1-0) and CO(2-1) line respectively. Each channel width could be slightly broader (by 10 or 20%) than the spacing of 1 MHz, degrading slightly the spectral resolution, but this is not critical, with respect to the half-power line width of at least $14\,km\,s^{-1}$ that we observed. The half power beam sizes at 115 and 230 GHz are $23''$ and $12''$. The observations were done using a nutating secondary, with a beamthrow of $\pm4'$ in azimuth. Pointing checks were done at least every two hours on nearby continuum sources and planets, with rms fluctuations of less than $3''$. The calibration of the receivers was checked by observing Galactic sources (Orion A and SgrB2).

The intensities are given here in T_A^*, the chopper wheel calibrated antenna temperature. To convert into main beam temperatures $T_{mb} = \frac{T_A^*}{\eta_{mb}}$ where η_{mb} is the main–beam efficiency. For the IRAM telescope η_{mb} is 0.60 and 0.45 for the CO(1-0) and CO(2-1) lines.

For NGC 628, we also combined a series of of CO(1-0) and CO(2-1) spectra obtained during the IRAM galaxy survey by Braine et al (1993). These were two radial cuts along the RA and DEC axis. In August 1994, we observed two radial cuts aligned along the major and minor axis of the galaxy, with a position angle 25° with respect to the previous cuts. We integrated about 30 min per point, and reached a noise level of about 15 mK and 30 mK for the CO(1-0) and CO(2-1) lines, at $2.6\ km\,s^{-1}$ resolution. We have smoothed the CO(2-1) data to $2.6\ km\,s^{-1}$ resolution to increase the signal-to-noise; according to the line-width observed (at least $10\ km\,s^{-1}$), this has never a significant broadening effect (less than 5%).

Some ^{13}CO spectra were also taken in November 1994 towards selected points in NGC 628, to test the effect of cloud overlap, and "macroscopic" optical depth of the ^{12}CO line on the derived line-width and velocity dispersion. The typical system temperatures were then 240 and 350 K at the ^{13}CO(1-0) and (2-1) (110 GHz and 220 GHz) respectively.
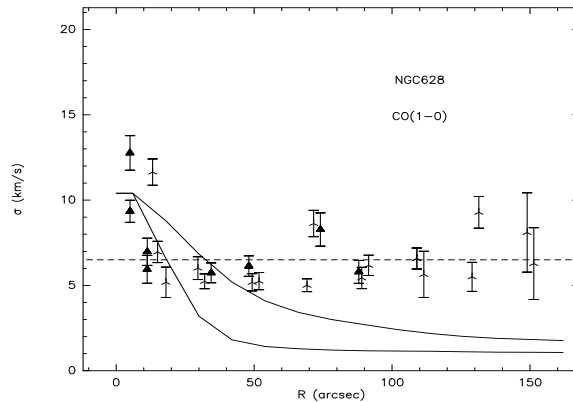

Fig. 5. Radial distribution of CO(1-0) velocity dispersions obtained through gaussian fits of the NGC 628 profiles. The points on the minor axis are marked by filled triangles. The full lines are the σ_v expected from an axisymmetric velocity models, where the width comes only from the beam-smearing of the rotational velocity gradients projected on the sky plane. The top line is for the minor axis, the bottom line for the major axis. The dashed horizontal line is the average value adopted for the ^{12}CO dispersion
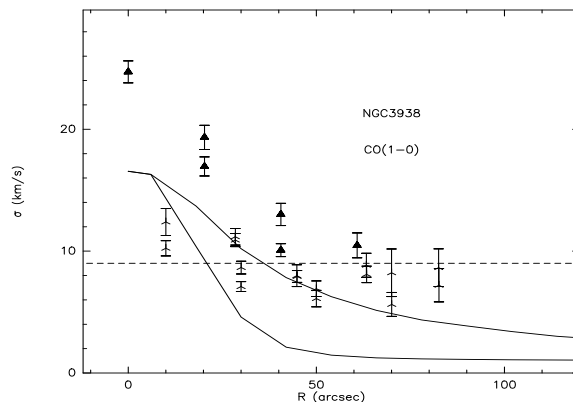

Fig. 6. Radial distribution of CO(1-0) velocity dispersions obtained through gaussian fits of the NGC 3938 profiles. Markers and lines as in previous figure.

4. Results

4.1. Spectra and radial distributions

An overview of the CO(1-0) spectra of the observed galaxies is shown in Figures 1 and 2. We derived the area, central velocity and velocity width of each profile through gaussian fits. Positions where the signal-to-noise ratio was not sufficient (below 3) were discarded. The radial distributions of integrated CO emission is displayed in figures 3 and 4, together with the derived rotation curves. The adopted positions angles and inclinations are those found

for the inner disk in H I by Kamphuis & Briggs (1992) for NGC 628, and and a compromise between the values from Bottema (1993) and van der Kruit & Shostak (1982) for NGC 3938. We minimised the dispersion by fitting the central CO velocity, which is indicated in Table 1.

4.2. Vertical velocity dispersion

The velocity dispersions, derived directly from the gaussian fits are displayed as a function of radius in figures 5 and 6 for NGC 628 and NGC 3938 respectively. The striking feature is the almost constancy of the velocity dispersion as a function of radius. The dispersion is slightly increasing towards the center, but this can be entirely accounted for by the rotational velocity gradients projected on the sky plane. We estimated these gradients for each position by modeling the radial distribution and velocity field of the molecular gas, assuming axisymmetry. The radial distribution was taken from the present observations: we fitted an exponential surface density model for the CO integrated emission, with an exponential scale-length of 6 kpc and 3 kpc respectively for NGC 628 and NGC 3938. This corresponds also to the radial distribution found by Adler and Liszt (1989) for NGC 628. We know that there might be a $10''$ (≈ 500 pc) hole in the NGC 628 center (Wakker & Adler 1995), corresponding to a hint of depletion in our CO(2-1) distribution; we have tested this in the model, and the effect on the expected beam-smoothed line-width was negligible. We also entered the values for the rotation curve obtained both from the inner H I disks (Shostak & van der Kruit 1984, van der Kruit & Shostak 1982), and the present CO rotational velocities. Both are compatible (cf fig. 3 and 4). We distributed randomly 4 10^4 test particules according to these radial distributions and kinematics, in a plane of thickness 100pc. No velocity dispersion of any sort was added, so that the spectrum of each particule is a delta function. After projection, and beam-smearing with a gaussian beam of $23''$ and $12''$ to reproduce the CO(1-0) and CO(2-1) respectively, the expected map of the velocity widths coming from in-plane velocity gradients was derived. The corresponding cuts along the minor and major axis are plotted in figures 5 and 6.

We see that in the center, the velocity width can sometimes be entirely due to the rotational gradients. This is not true for the outer parts, where the measured σ must represent the vertical velocity dispersion. These large effects of the rotational gradients explain the much larger line-widths found with a $45''$ beam by Young et al (1995); they also explain the spiral shape of the velocity residuals found in the H I kinematics by Foster & Nelson (1985), with comparable spatial resolution.

When trying to deconvolve the measued σ at the center, we obtain a rather flat profile of vertical velocity dispersion with radius. There are however some uncertainties: first, sometimes the expected gradient is larger
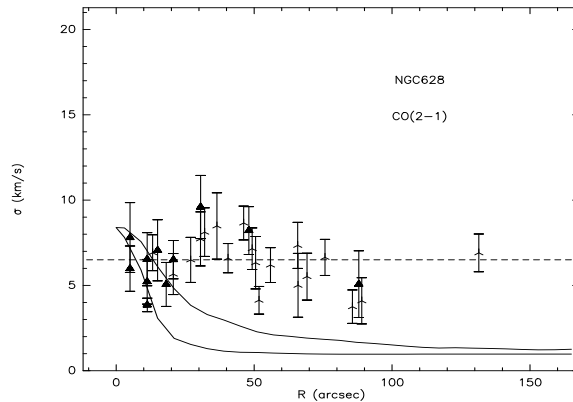

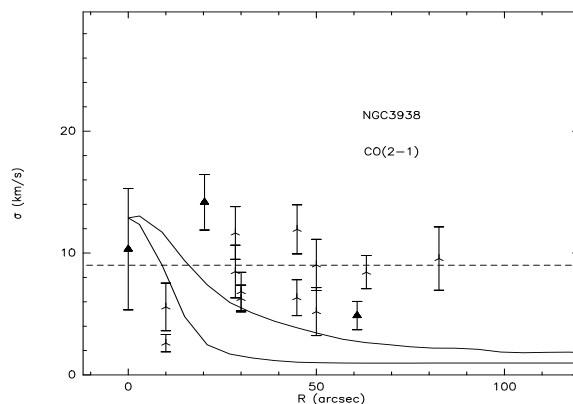**Fig. 7.** Same as fig 5 but for the CO(2-1) line.

Fig. 8. Same as fig 6 but for the CO(2-1) line.

than the observed one; this could be explained if the CO-emitting clouds are not spread all over the beam, and do not share the whole expected rotational gradients (for instance, if they are confined into arms). Also, the axisymmetric model might under-estimate the expected rotational gradients, since no streaming motions have been taken into account. We dont estimate it worth to refine the model, given the many sources of uncertainty.

The beam-smearing is less severe in the CO(2-1) line. The corresponding curves are plotted in fig 7 and 8. Unfortunately, the signal-to-noise ratio is lower for this line, due to both a higher system temperature, and a CO(2-1)/CO(1-0) emission ratio slightly lower than 1. The constancy of the line-width as a function of radius is however confirmed.

The constant value of the vertical dispersion $\sigma_v = $ (FWHM/2.35) is $6.5 \, \mathrm{km \, s^{-1}}$ and $9 \, \mathrm{km \, s^{-1}}$ for NGC 628 and NGC 3938 respectively. We can question the fact that this is not the true molecular gas dispersion, if there is a saturation effect in the ^{12}CO line, as shown by Garcia-Burillo

et al (1993). The less saturated ^{13}CO line profiles were found systematically narrower in the galaxy M51. To investigate this point, we observed a few ^{13}CO spectra, as shown in fig 9. We found indeed slightly narrower ^{13}CO line profiles, with a ^{12}CO/^{13}CO width ratio of 1.1 in average, in the (1-0) and the (2-1) lines as well. Only the (-17″,-16″) offset has a significantly higher ratio width of 1.35 (FWHM = 12.7 ±0.9 for the ^{12}CO line and FWHM=9.1 ± 0.7 for the ^{13}CO line). We can therefore conclude that the saturation effect is no more than 10% in order of magnitude in average over the galaxy, and we estimate the true velocity dispersion of the molecular gas perpendicular to the plane to be 6 km s^{-1} and 8.5 km s^{-1} for NGC 628 and NGC 3938.
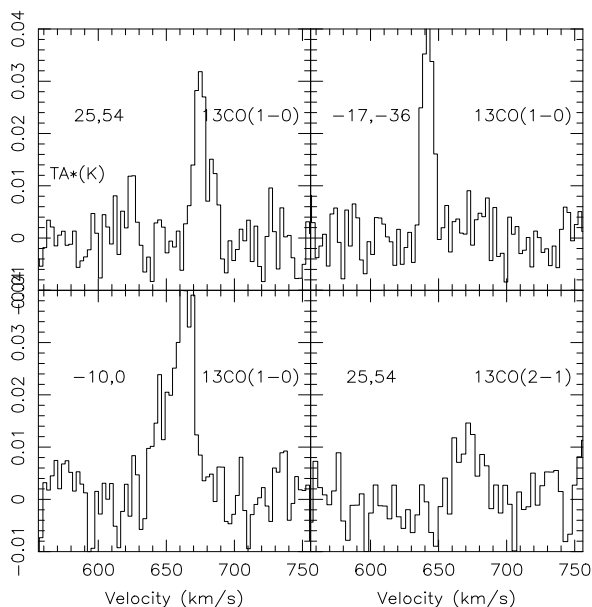

Fig. 9. Some ^{13}CO spectra taken towards NGC 628. The offsets are indicated at the top left, in arcsec.

4.3. Comparison of the two galaxies

It is interesting to compare the two galaxies NGC 628 and NGC 3938, since they are of the same type, and however the stellar surface density is about twice higher in NGC 3938, a property independent of the distance adopted (both the total luminosity and the characteristic radius are twice lower in NGC 3938). We can also note that the gas surface density is also twice higher in NGC 3938 (figure 10). How can we then explain that the vertical gas dispersion is higher in NGC 3938, while the stellar vertical dispersion is twice lower? First let us note that the maximum rotational velocities are comparable in the two

galaxies, and that is expected if they have similar M/L ratios: indeed the square of the velocity scales as M/R, which is similar for both objects. Now the critical velocity dispersions for stability in the plane scale as $\sigma_c \propto \mu/\kappa \propto \mu R/V$ and is also the same for both galaxies. We therefore expect the same planar dispersions, if they are regulated by gravitational instabilities. Since we observe a stellar vertical dispersion lower in NGC 3938, this means that the anisotropy is much higher in this galaxy.

For the self-gravitating stellar disk, we can apply the isothermal equilibrium, and find that the stellar scale-height h_* scales as σ_*^2/μ_* and should be 8 times smaller in NGC 3938. The stellar density in the plane ρ_0 should then be 16 times higher, and so should be the restoring force for the gas K_z. We can then deduce that the scale height of the gas is also smaller, but only by a factor 4 or less. In fact, there remains a free parameter, which is the vertical/planar anisotropy, which must result from the history of the galaxy formation and evolution (companion interactions, mergers, gas infall etc..) which should explain the differences between the two galaxies.

5. Summary and Discussion

One of the most important result is that the vertical velocity dispersion of the molecular gas in NGC 628 and NGC 3938 is constant as a function of radius. Morevover the value of this dispersion is $\sigma_v \approx$ 6-8 km s^{-1}, very comparable to that of the HI component.

This universality of the dispersion already tells us that it does not correspond to a thermal width. In that case, the dispersion is only a function of gas temperature, and this should vary with the galactocentric distance, since the cooling and heating processes depend strongly on the star formation efficiency. The temperature of dust derived from infra-red emission for instance, is a function of galactocentric radius. Also, the dispersion of the HI should then be very different from that of the colder molecular gas. It is clear at least for the cold molecular component that the line widths correspond to large-scale macroscopic turbulent motions between a large number of clumps of internal dispersion possibly much lower than 1 km s^{-1}.

The fact that the HI and CO emissions reveal comparable z-dispersions may appear surprising. It is well known from essentially our own Galaxy, that the HI plane is broader than the molecular gas plane, and this is attributed to a larger z-velocity dispersion (e.g. Burton 1992). In external galaxies, the evidence is indirect, because of the lack of spatial resolution. In M31, the comparison between HI and CO velocity dispersions led to the conclusion that the HI height was 3 or 4 times higher than the molecular one at R=18 kpc (Boulanger et al 1981). Is really the thin molecular component an independant layer embedded in a thicker HI layer? We discuss this further below.
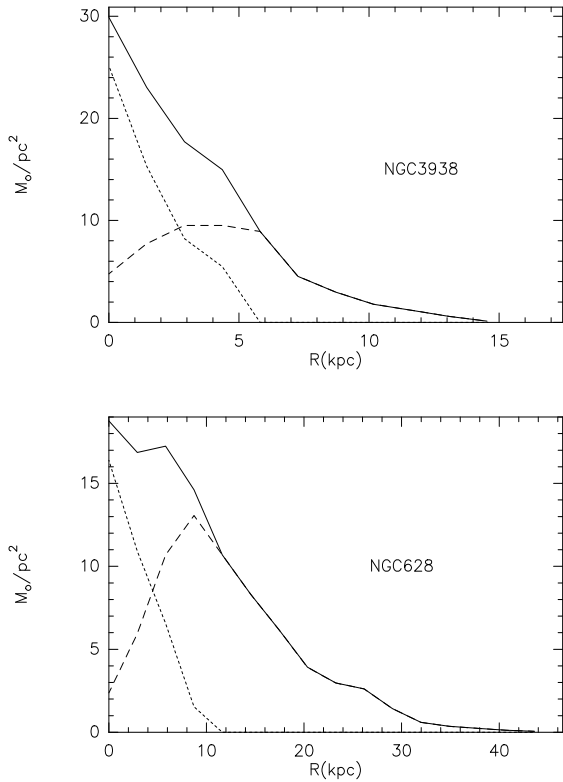
Fig. 10. Radial distributions of gas surface densities in NGC 628 (left) and NGC 3938 (right): H I (dash) and H$_2$ from CO (dots) are combined to estimate the total (full line) surface density. Helium is taken into account

5.1. Critical dispersion for gravitational stability

It is interesting to compare the observed vertical velocity dispersions to the critical dispersion required in the plane by stability criteria; as a function of gas surface density μ_g and epicyclic frequency κ, the critical dispersion can be expressed by (Toomre 1964):

$$\sigma_{cg} = 3.36 G \mu_g / \kappa$$

To obtain the total gas surface density μ_g, we have combined the available H I data (Shostak & van der Kruit 1984 for NGC 628; van der Kruit & Shostak 1982, for NGC 3938) to the present CO data as a tracer of H$_2$ surface density. We have multiplied the result by the factor 1.4, to take into account the helium fraction. We can see in figure 10 that the apparent central hole detected in H I is filled out by the molecular gas. This is not unexpected, since it is believed that above a certain gas density threshold, the atomic gas becomes molecular. This threshold involves essentially the gas column density, the pressure of the interstellar medium, the radiation field and

the metallicity, since the main point is to shield molecules from photodestruction (Elmegreen 1993). It is indeed observed that the average gas column density is sufficiently increasing towards the galaxy centers, to reach the threshold. Once the shielding conditions are met, the chemistry time-scale is short enough (of the order of 10^5 yrs) with respect to the dynamical time-scale, that the H I to H$_2$ phase transition occurs effectively. This transition is obvious in most galaxies (e.g. Sofue et al 1995, Honma et al 1995); the threshold at solar conditions for metallicity and radiation field is around 10^3 cm^{-3} and 10^{21} cm^{-2}, but it is difficult to precise it more because of spatial resolution effects, and because we rely upon CO emission to trace H$_2$ (the observed thresholds concern in fact CO excitation and photo-dissociation).

We have then built a mass model of the two galaxies in fitting their rotation curves, taken into account the constraints on the scale-lengths and masses of luminous components given by optical observations (section 2). In these fits, the gas contribution to the rotation curve have been found negligible. We include in the mass model a spherical bulge represented by a Plummer (size r$_b$, mass M$_b$), an exponential disk (scale-length h$_d$, mass M$_d$) and a flattened dark matter halo, represented by an isothermal, pseudo-ellipsoidal density (eg Binney & Tremaine 1987):

$$\rho_{DM} = \frac{\rho_{0,DM}}{\left(1 + \frac{r^2}{r_h^2} + \frac{z^2}{r_h^2 q^2}\right)}$$

where r_h is the characteristic scale of the DM halo and q its flattening. All parameters of the fits are displayed in Table 2. The fits are far from unique, but their essential use is to get an analytical curve fitting the observed rotation curve, in order to get derivatives and characteristic dynamical frequencies. Given the functional forms adopted for the various components, we can get easily the total mass, and compare the M/L with expected values for galaxies of the same types.

From these mass models, we have derived the epicyclic frequency as a function of radius (this does not depend on the precise model used, as long as the rotation curve is fitted), and the critical velocity dispersion required for axisymmetric stability, for the stellar and gaseous components (figures 11 and 12). The comparison with the observed vertical velocity dispersions for H I and CO is clear: the observed values are most of the time larger, in particular for NGC 3938. This means that, if the gas velocity dispersion can be considered isotropic, the Toomre stability parameter in the galaxy plane is always $Q_g \gtrsim 1$, and most of the time $Q_g > 2$-3, for NGC 3938. For NGC 628, Q_g is near 1 between 3 and 20kpc, and the threshold for star formation, $Q_g = 1.4$ according to Kennicutt (1989) is reached at 23 kpc. This is far in the outer parts of the galaxy, since R$_{25}$ = 15.5 kpc.

If the vertical dispersion is lower than in the plane, as could be the case (e.g. Olling 1995), than Q_g is even

Table 2. Mass models derived from rotation curve fits

Galaxy	NGC 628	NGC 3938
r_b(kpc)	1.5	0.8
$M_b(10^{10}$ $M_\odot)$	1.6	0.8
h_d(kpc)	3.9	1.75
$M_d(10^{10}$ $M_\odot)$	6.9	2.8
r_h(kpc)	14.	7.
$M_h(10^{10}$ $M_\odot)^*$	2.7	1.3
q	0.2	0.2
M(stars)/L_B	3.4	3.3
$M_{tot}(< R_{25})/L_B$	4.5	4.5

* Mass inside R_{25}=15.5 kpc for NGC 628 and 7.85 kpc for NGC 3938

larger. The gas appears then to be quite stable, unless the coupling gas-stars has a very large effect.

Figures 11 and 12 also plot the critical velocity dispersion for the stellar component, together with a fit to the observed stellar velocity dispersions, from van der Kruit & Freeman (1984) for NGC 628 and from Bottema (1988, 1993) for NGC 3938. From a sample of 12 galaxies where such data are available, Bottema (1993) concludes that the stellar velocity dispersion is declining exponentially as $e^{-r/2h}$, as expected for an exponential disk of scale-length h and constant thickness, as found by van der Kruit & Searle (1981). Since mostly the vertical stellar dispersion σ_z is measured, it is assumed that there is a constant ratio between the radial dispersion σ_r, comparable to that observed in the solar neighbourhood $\sigma_z/\sigma_r = 0.6$. This is already well above the minimum ratio required for vertical stability, i.e. $\sigma_z/\sigma_r = 0.3$ (Araki 1985, Merritt & Sellwood 1994). Within these assumptions, it can be derived that the Toomre parameter for the stars Q_* is about constant with radius, within the optical disk; it depends of course on the mass-to-light ratio adopted for the luminous component, and is in the range $Q_* \approx 1$ for M(stars)/$L_B = 3$. Figures 11 and 12 confirm the result of almost constant Q_*, but with low values, especially for NGC 3938. This could be explained, if the vertical dispersion is indeed much lower than the radial one. The minimum value for the ratio σ_z/σ_r is 0.3 (for stability reasons), so that the derived Q_* values displayed in figures 11 and 12 could be multiplied by ≈ 2. The idea of stellar velocity dispersion regulated by gravitational instabilities appears therefore supported by the data, within the uncertainties.

The most intriguing result is the large gas vertical dispersion observed for NGC 3938, and its distribution with radius. The large corresponding Q_g values, that will mean comfortable stability, are difficult to reconcile with the
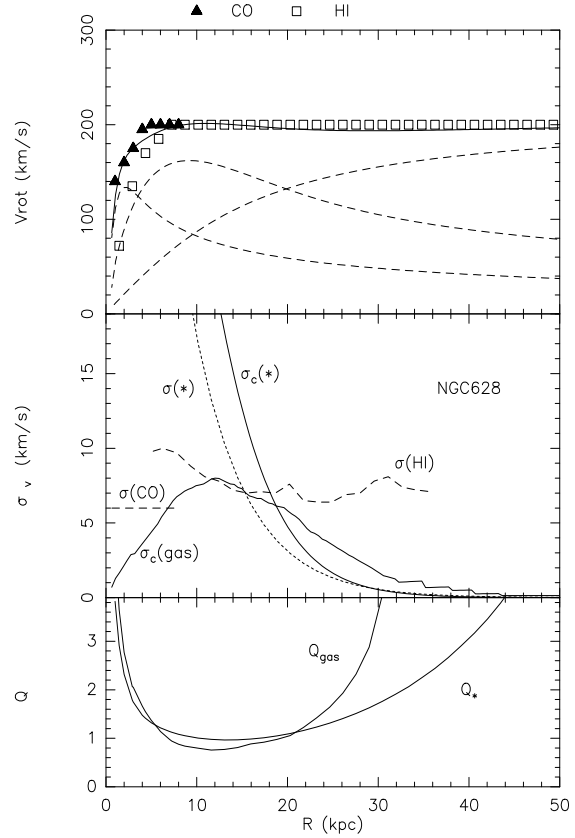

Fig. 11. Rotation curve fit for NGC 628: *top*: total fitted rotation curve (full line), with contributions of bulge, exponential disk and dark matter halo (dashed lines) compared with CO and H I data; *middle*: Derived critical velocity dispersions required for axisymmetric stability for stars and gas (full lines). The H I and CO observed vertical velocity dispersions are also shown for comparison (noted σ(HI) full line and σ(CO), horizontal dashed line). The H I dispersions data have been taken from the compilation in Kamphuis thesis (1992). A fit to the observed z-stellar velocity dispersion is also shown (σ(*), dotted line); *bottom*: Corresponding Toomre Q parameters, assuming σ_z/σ_r =0.6 for the stars (the CO dispersion has been taken for the gas)

observed large and small-scales gas instabilities: clear spiral arms are usually observed in the outer H I disks, with small-scale structure as well (see e.g. van der Hulst & Sancisi 1988, Richter & Sancisi 1994). This is also the case here for NGC 628 showing all signs of gravitational instabilities in its outer H I disk (Kamphuis & Briggs 1992), and for NGC 3938 (van der Kruit & Shostak 1982). A possibility to reduce Q_g is that also the gas dispersion is anisotropic, this time the vertical one being larger than in the plane. However we will see, through comparison with gas dispersion in the plane of the Galaxy (cf next section) that the anisotropy of gas dispersion does not appear
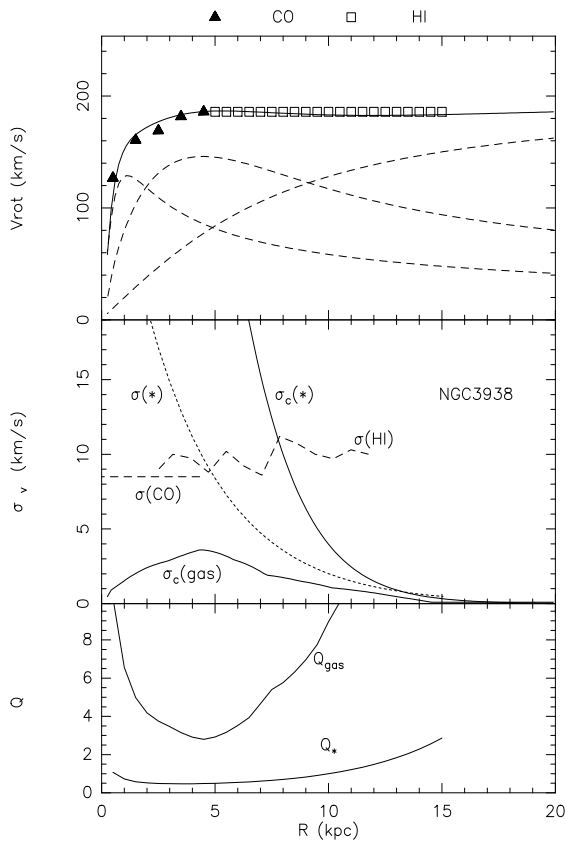
Fig. 12. Same as previous figure, for NGC 3938

so large. Another explanation could be that the present rough calculations of the Q-parameter concern only a simplified one-component stability analysis, and could be significantly modified by multi-components analysis. It has been shown (Jog & Solomon 1984, Romeo 1992, Jog 1992 & 1996) that the coupling between several components destabilises every dynamical component. The apparent stability ($Q \approx 2 - 3$) of the gas component might therefore not be incompatible with an instability-regulated velocity dispersion for the gas.

But then, in the vertical direction, the dispersion is much higher than the minimum required for vertical stability. Could this large velocity dispersion be powered by star formation? This is not likely, at least for the majority of the H I gas well outside the optical disk, where no stellar activity is observed. A possible explanation would be to suppose that the H I is tracing a much larger amount of gas, in the form of molecular clouds, which will then be self-gravitating, with $Q_g \lesssim 1$ (Pfenniger et al 1994; Pfenniger & Combes 1994). With a flat rotation curve, and a gas surface density decreasing as $1/r$, the critical dispersion would then be constant with radius.

5.2. Similar H I and CO vertical dispersions

5.2.1. Two phases of the same dynamical component

Another puzzle is the similarity of the CO and H I vertical velocity dispersions. If the gas layers are indeed isothermal in z, we can deduce that both atomic and molecular layers have also similar heights. This means that the atomic and molecular components can be considered as a unique dynamical component, which can be observed under two phases, according to the local physical conditions (density, excitation temperature, etc..). The amplitudes of z-oscillations of the molecular and atomic gas are the same, only we see the gas as molecular when it is at heights lower than ≈ 50pc. At these heights, the molecular fraction is $f_{mol} \gtrsim 0.8$ (Imamura & Sofue 1997), which means that almost all clouds are molecular, taking into account their atomic envelope. In fact it is not clear whether we see the CO or H_2 formation and destruction, since we can rely only on the CO tracer. Also, it is possible that the density of clouds at high altitude is not enough to excite the CO molecule, which means that the limit for observing CO will not be coinciding with the limit for molecular presence itself. The latter is strongly suggested by the observed vertical density profiles of the H_2 and H I number density: there is a sharp boundary where the apparent f_{mol} falls to zero, while we expect a smoother profile for a unique dynamical gas component.

That the gas can change phase from molecular to atomic and vice-versa several times in one z-oscillation is not unexpected, since the time-scale of molecular formation and destruction is smaller than the z-oscillation period, of $\approx 10^8$ yrs at the optical radius: the chemical time-scale is of the order of 10^5 yrs (Leung et al 1984, Langer & Graedel 1989). Morever, as discussed in the previous section (5.1), the key factor controlling the presence of molecules is photodestruction, which explains why there is a column density threshold above which the gas phase turns to molecular (Elmegreen 1993). This threshold could be reached at some particular height above the plane.

5.2.2. Collisions

Should we expect the existence of several layers of gas at different tmperatures, and therefore different thicknesses, in galaxy planes? In the very simple model of a diffuse and homogeneous gas, unperturbed by star-formation, we can compute the mixing time-scale of two layers at different temperatures, through atomic or molecule collisions: this is of the order of the collisional time-scale, $\approx 10^4$ yrs for an average volumic density of 1 cm^{-3}, and a thermal velocity of 0.3 km s^{-1}. This is very short with respect to the z-oscillation time scale of $\approx 10^8$ yrs, and therefore mixing should occur, if differential dissipation or gravitational heating is not taken into account.

This simple model is of course very far from realistic. We know that the interstellar medium, atomic as well as molecular, is distributed in a hierachical ensemble of clouds, similar to a fractal. Let us then consider another simple modelisation of an ideal gas where the particles are in fact the interstellar clouds, undergoing collisions (cf Oort 1954, Cowie 1980). For typical clouds of 1pc size, and 10^3 cm^{-3} volumic density, the collisional time-scale is of the order of 10^8 yrs, comparable with the vertical oscillations time-scale. This figure should not be taken too seriously, given the rough simplifications, but it corresponds to what has been known for a long time, i.e. the ensemble of clouds cannot be considered as a fluid in equilibrium, since the collisional time-scale is comparable to the dynamical time, like the spiral-arm crossing time (cf Bash 1979, Kwan 1979, Casoli & Combes 1982, Combes & Gerin 1985).

If the collisions were able to redistribute the kinetic energy completely, there should be equipartition, i.e. the velocity dispersion would decrease with the mass m of the clouds like $\sigma_v \propto m^{-1/2}$. In fact the cloud-cloud relative velocities are roughly constant with mass (between clouds of masses 100 M$_\odot$ and GMCs of 10^6 M$_\odot$, a ratio of 100 would be expected in velocity dispersions, which is not observed, Stark 1979). Towards the Galactic anticenter, where streaming motions should be minimised, the one-dimensional dispersion for the low-mass and giant clouds are found to be about 9.1 and 6.6 km s^{-1} respectively, with near constancy over several orders of magnitude, and therefore no equipartition of energy (Stark 1984). The almost constancy of velocity dispersions with mass requires to find other mechanisms responsible for the heating.

5.2.3. Gravitational heating

If relatively small clouds can be heated by star-formation, supernovae, etc...(e.g. Chièze & Lazareff 1980), the largest clouds could be heated by gravitational scattering (Jog & Ostriker 1988, Gammie et al 1991). In the latter mechanism, encounters between clouds with impact parameters of the order of their tidal radius in a differentially rotating disk are equivalent to a gravitational viscosity that pumps the rotational energy into random cloud kinetic energy. A 1D velocity dispersion of 5-7km s^{-1} is the predicted result, independent of mass. This value is still slightly lower than the observed 1D dispersion of clouds observed in the Milky Way. Stark & Brand (1989) find 7.8km s^{-1} from a study within 3 kpc of the sun. But collective effects, gravitational instabilities forming structures like spiral arms, etc... have not yet been taken into account. Given the high degree of structure and apparent permanent instability of the gas, they must play a major role in the heating, the source of energy being also the global rotational energy. Dissipation lowering the gas dispersion continuously maintains the gas at the limit of instability, closing the feedback loop of the self-regulation (Lin & Pringle 1987,

Bertin & Romeo 1988). In the external parts of galaxies, where there is no star formation, gravitational instabilities are certainly the essential heating mechanism. This again will tend to an isothermal, or more exactly isovelocity, ensemble of clouds, since the gravitational mechanism does not depend on the particle mass. The molecular or atomic gas are equivalent in this process, and should reach the same equilibrium dispersion.

5.2.4. H I and CO velocity dispersions in the Milky Way

In the Milky Way, although the kinematics of gas is much complicated due to our embedded perspective, we have also the same puzzle. The velocity dispersion has been estimated through several methods, with intrinsic biases for each method, but essentially the dispersion has been estimated in the plane. Only with high-latitude molecular clouds, can we have an idea of the local vertical velocity dispersion. Magnani et al (1996) have recently made a compilation of more than 100 of these high-latitude clouds. The velocity dispersion of the ensemble is 5.8km s^{-1} if seven intermediate velocity objects are excluded, and 9.9 km s^{-1} otherwise. This is interestingly close to the values we find for NGC 628 (6km s^{-1}) and NGC 3938 (8.5km s^{-1}). Unfortunately there is always some doubt in the Galaxy that all molecular clouds are taken into account, due to many selection effects, while the measurement is much more direct at large scale in external face-on galaxies. In fact, it has been noticed by Magnani et al (1996) that there were an inconsistency between the local measured scale-height of molecular clouds (about 60pc) and the vertical velocity dispersion. However, they conclude in terms of a different population for the local high-latitude clouds (HLC). Indeed, the total mass of observed HLC is still a small fraction of the molecular surface density at the solar radius.

The local gaussian scale height of the molecular component has been derived to be 58pc (at R$_\odot$ = 8.5kpc) through a detailed data modelling by Malhotra (1994); this is also compatible with all previous values (Dame et al 1987, Clemens et al 1988). The local H I scale height is 220pc (Malhotra 1995). We therefore would have expected a ratio of 3.8 between the dispersions of the H$_2$ and H I gas, but these are very similar, within the uncertainties, which come mainly from the clumpiness of the clouds for the H$_2$ component. If we believe the more easily determined H I dispersion of 9km s^{-1} (Malhotra 1995), then the H$_2$ dispersion is expected to be 2.4km s^{-1}, clearly outside of the error bars or intrinsic scatter: the value at the solar radius is estimated at 7.8km s^{-1} by Malhotra (1994). Of course, all this discussion is hampered by the fact that we discuss mainly horizontal dispersions in the case of the Milky Way, while the gas dispersions could well be anisotropic. This is why the present results on external face-on galaxies are more promising.

The vertical gas velocity dispersion in spiral galaxies is an important parameter required to determine the flattening of the dark matter component, combined with the observation of the gas layer thickness (cf Olling 1995, Becquaert & Combes 1997). We have shown here that the gas dispersion does not appear very anisotropic, in the sense that the vertical dispersion is not much smaller that what has been derived in the plane of our Galaxy (for instance by the terminal velocity method, Burton 1992, Malhotra 1994). Such vertical dispersion data should be obtained in much larger samples, to consolidate statistically this result.

References

Adler D.S., Liszt H.S.: 1989, Ap.J. 339, 836

Araki S.: 1985, PhD Thesis, Massachussetts Institute of Technology

Bash F.H.: 1979, ApJ 233, 524

Becquaert J-F., Combes F.: 1997, A&A in press

Bertin G., Romeo A.: 1988, A&A 195, 105

Binney, J. & Tremaine, S. 1987, "Galactic Dynamics", Princeton University Press, Princeton, New Jersey

Bosma A.: 1981, AJ 86, 1971

Bottema R.: 1988, A&A 197, 105

Bottema R.: 1993, A&A 275, 16

Boulanger F., Stark A.A., Combes F.: 1981, A&A 93, L1

Braine J., Combes F., Casoli F. et al : 1993 A&AS 97, 887

Brinks E., Burton W.B.: 1984, A&A 141, 195

Briggs F.H., Wolfe A.M., Krumm N., Salpeter E.E.: 1980, ApJ 238, 510

Burton W.B.: 1992, in "The Galactic Interstellar medium", SAAS-FEE Advanced Course 21, ed. D. Pfenniger & P. Bartholdi, Springer-Verlag, p. 1

Casoli F., Combes F.: 1982, A&A 110, 287

Chièze J.P., Lazareff B.: 1980, A&A 91, 290

Clemens D.P., Sanders D.B., Scoville N.Z.: 1988, ApJ 327, 139

Combes F., Gerin M.: 1985, A&A 150, 327

Cowie L.L.: 1980, ApJ 236, 868

Dame T.M., Ungerechts H., Cohen R.S. et al 1987, ApJ 322, 706

Danver C.G.: 1942, Ann. Obs. Lund 10

Dickey J.M., Hanson M.M., Helou G.: 1990, Ap.J. 352, 522

Elmegreen B.G.: 1993, ApJ 411, 170

Foster P.A., Nelson A.H.: 1985, MNRAS 215, 555

Gammie C.F., Ostriker J.P., Jog C.J.: 1991, ApJ 378, 565

Garcia-Burillo S., Combes F., Gerin M.: 1993, A&A 274, 148

Honma M., Sofue Y., Arimoto N.: 1995, A&A 304, 1

Imamura K., Sofue Y.: 1997, A&A 319, 1

Jog C., Ostriker J.P.: 1988, ApJ 328, 404

Jog C., Solomon P.M.: 1984, ApJ 276, 114 & 127

Jog C.: 1992, ApJ 390, 378

Jog C.: 1996, MNRAS 278, 209

Kamphuis J.: 1992, PhD thesis, Groningen Univ.

Kamphuis J., Briggs F.: 1992, A&A 253, 335

Kennicutt R.C.: 1989, ApJ 344, 685

Kwan J.: 1979, ApJ 229, 567

Langer W.D., Graedel T.E.: 1989, ApJS 69, 241

Leung C.M., Herbst E., Huebner W.F.: 1984, ApJS 56, 231

Lin D.N.C., Pringle J.E.: 1987, ApJ 320, L87

Magnani L., Hartman D., Speck B.G.: 1996, ApJS 106, 447

Malhotra S.: 1994, ApJ 433, 687

Malhotra S.: 1995, ApJ 448, 138

Merrifield M.R.: 1992, AJ 103, 1552

Merritt D., Sellwood J.A.: 1994, ApJ 425, 551

Natali G., Pedichini F., Righini M.: 1992, A&A 256, 79

Olling, R. P. 1995, AJ 110, 591

Oort J.H.: 1954, Bull Astron. Inst. Neth. 12, 177

Pfenniger, D. Combes, F. , Martinet, L. 1994, A&A 285, 79

Pfenniger, D. & Combes, F. 1994, A&A 285, 94

Richter O., Sancisi R.: 1994, A&A 290, L9

Romeo A.B.: 1992, MNRAS 256, 307

Rubin V.C., Burstein D., Ford W.K., Thonnard N.: 1985, ApJ 289, 81

Sandage A., Tamman G.A.: 1974, ApJ 194, 559

Sandage A., Tamman G.A.: 1975, ApJ 196, 313

Shostak G.S., van der Kruit P.C.: 1984, A&A 132, 20

Sofue Y., Honma M., Arimoto N.: 1995, A&A 296, 33

Stark A.A.: 1979, PhD Thesis, Princeton U.

Stark A.A.: 1984, ApJ 281, 624

Stark A.A., Brand J.: 1989, ApJ 339, 763

Toomre A: 1964, ApJ 139, 1217

van der Huslt T., Sancisi R.: 1988, AJ 95, 1354

van der Kruit P.C., Searle L.: 1981, A&A 95, 105

van der Kruit P.C., Shostak G.S.: 1982, A&A 105, 351

van der Kruit P.C., Shostak G.S.: 1984, A&A 134, 258

van der Kruit P.C., Freeman K.C.: 1984, ApJ 278, 81

Vogel S.N., Rand R.J., Gruendl R., Teuben P.: 1993, PASP 105, 666

Wakker B.P., Adler D.S.: 1995, AJ 109, 134

Young J.S., Xie S., Tacconi L. et al.: 1995, ApJS 98, 219